Oxidation of NO to NO_2 with Ozone in Real Flue Gas Emitted from a Diesel Oil Combustor

Punya Promhuad[1,4], *Kampanart* Theinnoi[2,4], *Thawatchai* Wongchang[3,4], *Phurin* Chonpan[2], *Teerapong* Iamcheerangkoon[2], and *Sak* Sittichompoo[2,4*]

[1]Techno Park, King Mongkut's University of Technology North Bangkok, 10800 Bangkok, Thailand
[2]Department of Power Engineering Technology, College of Industrial Technology, King Mongkut's University of Technology North Bangkok, 10800 Bangkok, Thailand
[3]Department of Mechanical and Automotive Engineering Technology, Faculty of Engineering and Technology, King Mongkut's University of Technology North Bangkok, (Rayong Campus), 21120 Rayong, Thailand
[4]Research Centre for Combustion Technology and Alternative Energy (CTAE), King Mongkut's University of Technology North Bangkok, 10800 Bangkok, Thailand

Abstract. To reduce nitrogen oxides emissions (NOx) from flue gas, selective catalytic reduction (SCR) or adsorption using various solution are efficient methods. However, nitric oxide (NO) needs to be oxidised into nitrogen dioxide (NO_2) to enhance NOx removal performance. This paper presents the effects of operating parameter of a dielectric barrier discharge (DBD) reactor on ozone (O_3) generation which ozone was utilised to oxidise NO into NO_2 in the real flue gas from diesel oil burner. A cylindrical DBD configuration with 1.5 mm electrode gap and effective discharge volume ranged from 13.8 cm^3 were chosen to produce O_3-rich air for oxidising NO. Using concentrated O_2 instead of air as O_3 source could enhance O_3 formation (8.57 g/kWh vs. 44.08 g/kWh). NO conversion to NO_2 by O_3 was strongly dependent on O_3/NO ratio. Additionally, thermal O_3 decomposition by heat energy in flue gas also substantially reduced O_3 which must be compensated by using excess O_3/NO ratio. At flue gas temperature of 407°C, O_3/NO ratio of 6.37 was required to complete oxidise NO into NO_2. The optimal NO conversion efficiency of 2.93 g/kWh was realised at flue gas resident time of 313 ms and flue gas temperature of 483°C.

1 Introduction

Rapid Combustion of carbon-containing fuel (e.g. fossil fuels) has been the main source of carbon emissions such as carbon dioxide (CO_2) which associates with greenhouse effect that raises global surface temperature [1]. The rise of average global temperatures leads to extreme patterns of climate which adversely affect environment, ecosystem, and quality of life. Nitrogen oxides (NOx) is another air pollutant that emitted from complete combustion as the result of Thermal NOx [2]. High nitrogen-containing fuel could also produce high level of NOx emission [3] through fuel-NOx and prompt-NOx pathways [4]. High concentration of NOx emitted into the atmosphere results in acid rain which causes corrosion to buildings, and anything made from metals. It is of importance to manage the level of NOx to mitigate the negative consequences.

Selective catalytic reduction (SCR) [5] is a well-established aftertreatment technology for NOx reduction. SCR operates by injecting reagent (e.g. ammonia (NH_3) or urea ($((NH_2)_2CO)$)) which reduces NOx into N_2 and H_2O through $4NH_3 + 4NO + O_2 \rightarrow 6H_2O + 4N_2$ and $4NH_3 + 2NO_2 + O_2 \rightarrow 6H_2O + 3N_2$ reactions [6]. However, these reactions proceed at slow pace and take relatively extended duration to complete compared to $4NH_3 + 2NO + 2NO_2 \rightarrow 6H_2O + 4N_2$ reaction which is known as 'fast-SCR' reaction [7]. Fast SCR reaction takes approximately 1 s or shorter to complete, hence; the process is more likely to complete within the catalyst. To achieve fast SCR reaction, the ratio between NO_2 to NO (NO_2/NO ratio) must equal to unity [8]. However, for flue gas from liquid and solid fuels combustion, NO is the only gas species emitted. Therefore, it is crucial to increase the NO_2/NO ratio which can be performed by oxidising NO into NO_2.

NO can be oxidised with O_2 in the presence of platinum (Pt) catalyst [9] via the general reaction: $NO + O_2 \rightarrow NO_2$. Even though, NO to NO_2 conversion could take place from 90 to 500°C, but conversion efficiency trends to reduce as gas temperature increase. Furthermore, conversion efficiency of catalytic process reaches approximately 60 % at 350 °C due to the nature of oxidation catalyst. On the other hand, NO can be effectively oxidised into NO_2 using O_3 [10] via $NO + O \rightarrow NO_2$ and $NO + O_3 \rightarrow NO_2 + O_2$ reactions [11]. In general, dielectric barrier discharge (DBD) [12, 13] is the most common O_3 generation method which utilises high voltage (HV) electricity to convert oxygen into ozone. Air is the most universal feedstock for ozone production due to the abundance availability. However, ozone yield and ozone efficiency are lower than using higher oxygen concentration mixture or pure oxygen as feedstock [14] due to ozone decomposition by catalytic reactions of NO

* Corresponding author: sak.s@cit.kmutnb.ac.th

 https://doi.org/10.1051/e3sconf/202567901002

and NO_2 [11]. Overall, ozone injection technique is a practical method to oxidise NO into NO_2 on-site where high conversion efficiency and low maintenance are important aspects of implementation.

The interaction between NO and O_3 is well documented [15-17]. However, most preliminary studies were conducted at laboratory-scale using simulated flue gas [15] or only NO, O_2, and N_2 mixtures [18]. Many studies conducted the experiment without the presence of water [19], small experiment scale [17], low gas temperature [18], and long residence time [20]. It is important to understand the effect of the abovementioned parameters which are encountered in real-world situations e.g. moisture content, sulphur, particles, short residence time, high temperature, and larger system's scale. Therefore, the experimental investigation with real flue gas at elevated flow rate will reduce the gap between theoretical studies and the actual application of ozone injection technique.

This paper presents an experimental investigation of a step-up scale of NO oxidation from small diesel oil burner using ozone injection to promote NO_2 formation. Our work investigates the effects of ozone production parameters (e.g. high voltage discharge voltage and frequency, inlet feed oxygen concentration) on the characteristics of ozone-rich air and the effects residence time and flue gas temperature on NO oxidation process.

2 Material and methods

2.1 Ozone production from DBD reactor

For DBD reactor employed in this study, most metal parts were fabricated from stainless steel 304 using multiple DBD cells connected in parallel in the same configuration experimented in [21] and [22]. Although, the main different was the material of the dielectric barrier which borosilicate glass tubes with outer diameter of 23 mm and glass tube wall thickness of 1.5 mm were used as dielectric barrier which mounted with inner electrodes. The gap between outside the dielectric barrier and outer electrodes was 1.5±0.5 mm. The total number of DBD cell was 12 cells which resulted in effective discharge volume of 13.8 cm^3. Dry air and bottled oxygen (99.99%) were used as oxygen source for ozone production. Feed air flow rate was regulated by a mass flow controller (MFC) (SMC model (PF2A750 – F02 - 27) at fixed flow rate of 20.0 LPM. A Trek 10/10B-HS high voltage power supply (HVPS) was used to produce high voltage (HV) electricity for the DBD reactor. The Trek HVPS's output signal was controlled by square wave generated by a Keysight DSOX1204 digital storage oscilloscope which also monitored the output HV voltage and current for calculating discharge electrical power. In this study, discharge voltage between 7 to 10 kV (peak) and discharge frequency between 100 to 500 Hz were used during the experiment. Figure 1 illustrates the discharge waveform monitored by Trek 10/10B-HS's outputs which depicts the phase shift of current profile compared to that of discharge voltage profile. The leading phase shift observed in the discharge current is indicative of a capacitive load, which arises from the inherent geometric configuration of the DBD reactor. This is the feature that is commonly observed in typical ozoniser [23]. Specific energy density (SED) between 425 - 996 J/L were used which could be written as the ratio of electric input power (P_{in} in W) to DBD reactor inlet air mixture flow rate ($\dot{V}_{air}$ in LPM) as shown in equation (1).

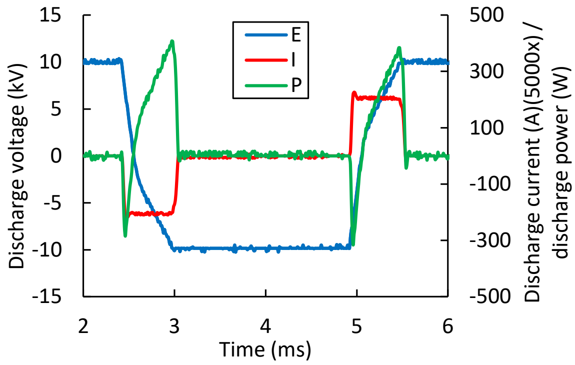

Fig. 1. DBD waveform at 10 kV_{peak}/ 600 Hz.

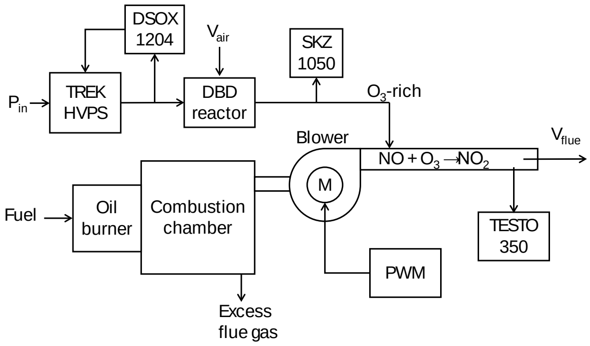

Fig. 2. Schematic diagram of experiment setup.

$$SED = 60 \times \frac{P_{in}}{\dot{V}_{air}} \quad (1)$$

A SKZ 1050-O_3 portable analyser was utilised to quantify the amount of O_3 generated from the DBD reactor. Hence, ozone production rate ($\dot{m}_{ozone}$, g/h) could be calculated by equation (2). Where ρ is ozone density (g/L) at a given temperature and pressure, and C is ozone concentration in (ppm-vol).

$$\dot{m}_{ozone} = 60 \times \rho \times \dot{V}_{air} \times \frac{C}{1000000} \quad (2)$$

To quantify the amount of ozone produced per one unit of electricity, specific ozone production (SOP) (in g/kWh) is depicted in equation (3). Where P_{in} represents the total electrical input power of the high voltage power supply system (HVPS and DSOX1204) measured by a power meter.

$$SOP = \dot{m}_{ozone} \times \frac{1000}{P_{in}} \quad (3)$$

2.2 Oxidation of NO in flue gas using ozone

Diesel oil burner, Olympia SL-3LP, was operated with 30% excess air with mean diesel fuel flow rate of 5.54 kg/h generated flue gas containing gas compositions as shown in Table 1. Gas species in the flue gas stream such as NO, NO_2, CO, CO_2, and O_2 were volumetrically quantified by a Testo 350 flue gas analyser.

Table 1. Baseline flue gas compositions (volumetric).

NO (ppm)	NO_2 (ppm)	CO (ppm)	CO_2 (%)	O_2 (%)
55.4	1.7	12.24	11.3	5.01

The turbine side of an automotive turbocharger was mechanically coupled to a DC motor to form an in-house built flue gas blower. Flue gas flow rate ($\dot{V}_{flue}$) was regulated by controlling the DC motor using pulse width modulation (PWM) technique. Tracer gas method [24] was used to measure the flue gas flow rate. Four different flue gas flow rates were experimented which resulted in 250 to 831 ms residence time for reaction between NO and O_3 to form NO_2. Residence time of NO and O_3 was the reciprocal of GHSV (Gas Hourly Space Velocity) as shown in equation (4) where volume of reactor is the volume of pipe section between O_3 injection port and Testo350 sampling port. Figure 2 illustrates the experimental setup utilised in this experimental investigation.

$$Residence\ time = GHSV^{-1} = \left(\frac{\dot{V}_{gas}}{V_{reactor}}\right)^{-1} \qquad (4)$$

3 Results and discussions

3.1 Ozone production characteristics of DBD reactor

Figure 3 illustrates the concentration of O_3 and NO_2 at the outlet of the DBD reactor for operating duration of 900 seconds (15 minutes) with dry air as feedstock. The chart reveals that O_3 and NO_2 concentrations started to increase 60 seconds after the HVPS was turned on. Subsequently, the concentrations of O_3 and NO_2 rapidly increased until the 400th second, while the HVPS input power sharply declined. NO_2 is formed after O_3 formation based on high O_3/NO_2 ratio during early operation of HVPS which suggests that O_3 was generated first from oxygen in air via $O_2 + e \rightarrow 2O + e$ and $O + O_2 \leftrightarrow O_3$ reactions. Then, NO was produced through $N_2 + O \leftrightarrow NO + N$ reaction. Simultaneously, HV discharge also generated N via $N_2 + e^- \rightarrow 2N$ reaction which acted as a precursor for NO formation through $N + O_2 \leftrightarrow NO + O$ reaction. In this case, the absence of H_2O in dry air inhibited the formation of NO via OH + N pathway. The high O_3 concentration (O_3/NO >= 1 [25]) favoured NO oxidation into NO_2 through $NO + O_3 \rightarrow NO_2 + O_2$ and $NO + O \rightarrow NO_2$ reactions [22]. Due to substantial concentrations of O_3, no trace of NO was detected as the entire NO was converted into NO_2. It is reasonable to infer that $O + O_2 \leftrightarrow O_3$ and $NO + O_3 \rightarrow NO_2 + O_2$ reactions are ozone-consuming process that limits ozone yield in addition to the gas temperature increased by joules-heating phenomenon [26]. It can be observed that O_3/NO_2 ratio reached near steady-state around the value 1.9 after HVPS operated approximately 300 seconds. No significant change of O_3/NO_2 ratio was observed indicating the limit of O_3 production.

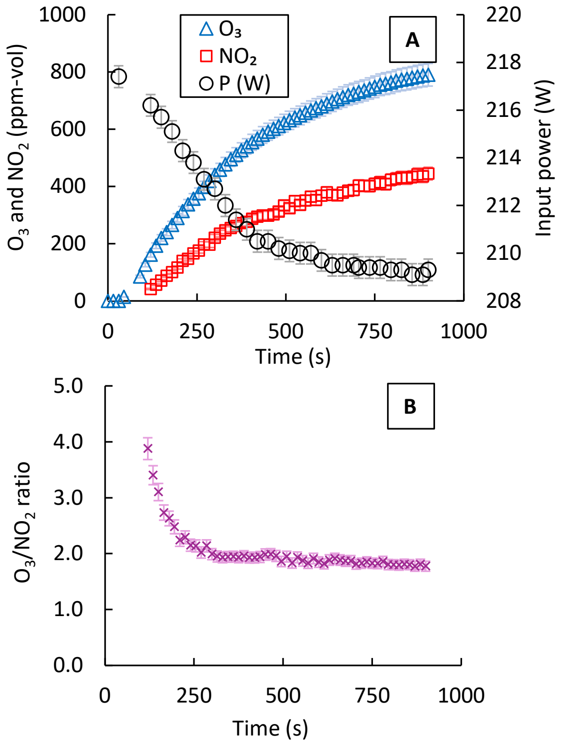

Fig. 3. Time evolution of O_3 and NO_2 production, and O_3/NO_2 ratio from DBD reactor at 10kV and 200 Hz.

As ozone generation progressed, HVPS input power started to decline which was due to the convergence toward equilibrium of gas compositions within discharge zone of the DBD reactor. The compositions of gases within the DBD reactor were believed to substantially influences the capacitance and the equivalence series resistance of the DBD reactor. Assuming the inductance of the circuit remains constant, a reduction in capacitance led to an increase in the capacitive reactance (X_c) of the DBD reactor, as defined by $X_C=(2\pi fC)^{-1}$. The elevated reactance imposed greater impedance to current flow, thereby attenuating the discharge current and consequently resulted in a decrease in the input power of the HVPS.

Figure 4 depicts the effect of HVPS operating frequency on O_3 and NO_2 production characteristics which higher discharge frequency increases number of discharge repetition in given period. As the result, more oxygen (O) and nitrogen (N) radicals could be generated which linearly enhanced ozone production rate as illustrated in Fig.4A. Similarly, the radical N and O facilitated the formation of NO which subsequently oxidised into NO_2 in an overall linear trend similar to that of O_3. Although, O_3 and NO_2 concentrations appeared to increase concurrently, a slight declined of O_3/NO_2 ratio (Figure 4B) at higher discharge frequency indicates that O_3 production rate increased less rapidly than the rate of NO_2 formation. The formation of NO_2 in the context of O_3 production is considered undesirable because it diverts energy away from dissociation of O_2 molecules and decreases the efficiency of O_3 production. Figure 4C illustrates that ozone yield increases with higher discharge frequency as the results of greater number of times of energy injection to feed gas per given duration [13]. It should be noted that the ozone yield reported in this study may appear lower compared to values presented in literature reviews (in the "introduction" section). This discrepancy arises from the differing methodologies used to measure electrical power. In this work, ozone yield was calculated based on the total input power of the system, which accounts for all energy losses. Consequently, the results presented here offer a realistic assessment of system performance and are directly applicable for scaling purposes in future implementations utilising this dataset.

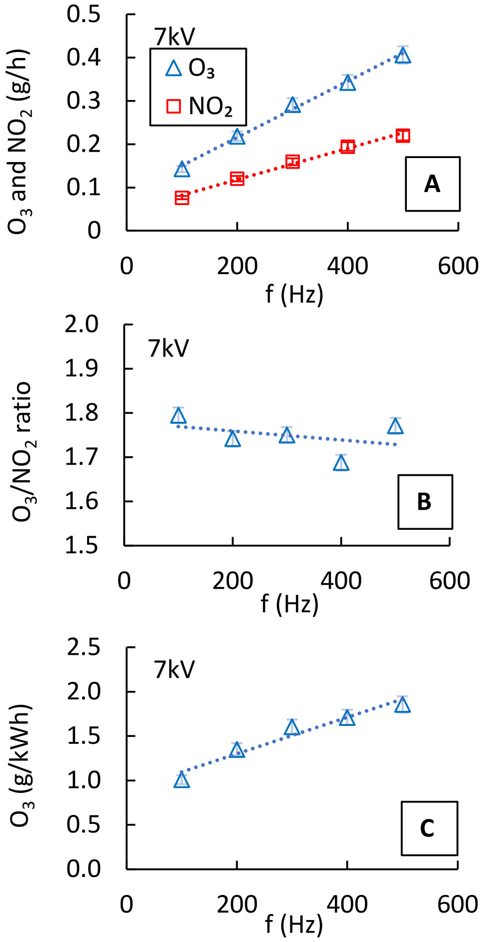

Fig. 4. Effect of discharge frequency and voltage on O_3 and NO_2 productions, O_3/NO_2 ratio, and O_3 yield.

On the other hand, Figure 5A demonstrates the effect of HVPS supply voltage on O_3 and NO_2 production characteristics. Overall, increasing discharge voltage seemed to exhibit similar effect on O_3 production rate as increasing the discharge frequency by effectively increase energy into the O_2 dissociation process. Increasing discharge voltage enhanced specific energy density applied to air feedstock which raised input energy for O_2 and N_2 excitation to produce O and N radicals and resulted in higher O_3 and NO_2 concentrations in product mixture. The O_3/NO_2 ratio in Figure 5B demonstrates different trend to that of Fig.4B which O_3/NO_2 increases from 1.8 toward 1.9 with higher discharge voltage. The results reveal that increasing discharge voltage had significant impact on O_3 generation at given discharge frequency. In this scenario, the increase discharge voltage led to the rate of O_3 formation exceeded that of NO_2, which is considered advantageous for optimising the ozone generation process. Figure 5C displays that O_3 yield rose from approximately 2 g/kWh to 7 g/kWh when increased discharge voltage from 7 to 10 kV. This indicates that discharge voltage played a significant role in ozone production efficiency. Nevertheless, the discharge voltage is fundamentally constrained by the dielectric strength of the insulation materials used within the high-voltage circuitry, including the ceramic insulator employed in the DBD reactor. Increasing the discharge voltage necessitates a larger reactor geometry and results in greater overall system weight. Thus, while higher discharge voltages may enhance ozone yield, they do so at the expense of increased reactor size, weight, and component costs required to withstand elevated electrical stresses. Ozone yield obtained by using air as oxygen feedstock reached a maximum value of 7 g/kWh at 10 kV and 500 Hz in this study.

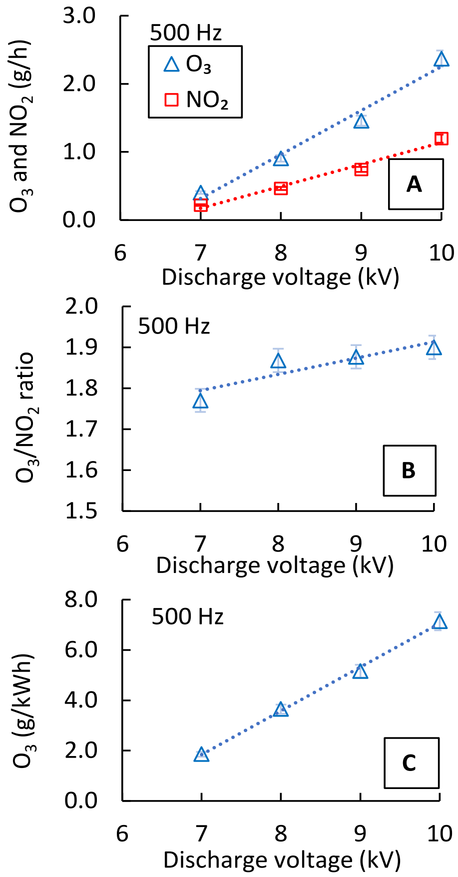

Fig. 5. Effect of discharge frequency and voltage on O_3 and NO_2 productions, O_3/NO_2 ratio, and O_3 yield

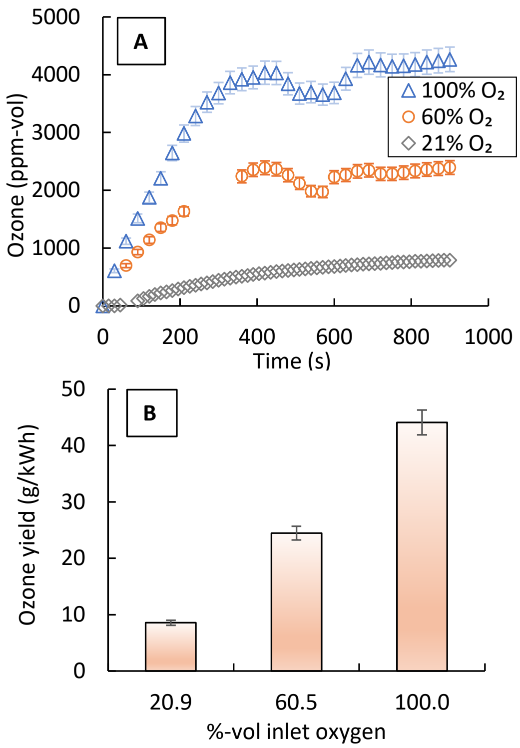

Fig. 6. Time evolution of different air feed oxygen concentrations on ozone production (A), and ozone yield (B) from DBD reactor at 10kV and 200 Hz.

Figure 6A illustrates the concentration of O_3 and NO_2 at the outlet of DBD reactor when different inlet O_2 concentrations applied over 900 seconds with discharge voltage and frequency of 10 kV and 200 Hz, respectively. The higher O_2 concentrations in feed air resulted higher O_3 concentrations due to greater chance of collision between free electrons and oxygen molecules. O_3 concentrations climbed up sharply during the first 300 seconds after HVPS was operated and reached the first peak around 400th second for both 60.5% and 100% O_2 feeds. However, a noticeable O_3 concentration fluctuation can be observed which followed by a steady increase and the concentration started to plateau soon after. The fluctuation was thought to occur as the result of unstable flow rate of oxygen flow controller which such a pattern persisted for both 60.5% and 100% O_2 feed conditions. At 900th second, ozone concentration of 784, 2392, and 4241 ppm-vol were observed with inlet O_2 feed of 21%, 60.5%, and 100%, respectively. The data indicate a positively correlated, slightly superlinear relationship between inlet oxygen concentration and outlet ozone concentration. Specifically, a 2.88-fold increase in oxygen concentration (from 21% to 60.5%) resulted in a 3.05-fold increase in ozone output concentration (784ppm→2392ppm), while a 4.76-fold increase in oxygen inlet concentration (from 21% to 100%) led to a 5.41-fold increase in ozone outlet concentration (784ppm→4241ppm). These findings suggest that the efficiency of ozone formation improves with higher oxygen availability, potentially due to enhanced reaction kinetics or reduced energy losses in the HV discharge process. The exclusion of N_2 from the input feed contributed to the enhanced O_3 yield, as it allowed the HV discharge energy to be fully directed toward the dissociation of oxygen molecules for ozone formation. In the absence of N_2, energy is not diverted toward the formation of NO_2, an undesired byproduct, thereby improving the overall efficiency of the ozone generation process. As shown in Figure 6B, an increase in oxygen concentration from 21% to 60.5% resulted in a sublinear enhancement of ozone yield, with a 2.85-fold increase from 8.57 g/kWh to 24.46 g/kWh. In contrast, elevating the oxygen concentration from 21% to 100% produced a mildly superlinear response, yielding a 5.14-fold increase in ozone output, reaching 44.08 g/kWh. These observations underscore the critical role of oxygen purity in maximizing ozone production efficiency of a DBD reactor. However, the energy requirements associated with generating high-purity oxygen must be carefully considered to assess the practical viability of employing enriched oxygen feeds in real-world applications.

3.2 Oxidation of NO in real flue gas using ozone

After the ozone generation characteristics have been established, a diesel oil burner was operated and allowed to heat up and reached a steady state which flue gas temperature and compositions were approximately constant. Ozone flow rate between 0.88 to 4.74 g/h was injected into flue gas stream 80 cm upstream the sampling port which was corresponding to approximately 13 times of the flue gas pipe inside diameter. This was done to ensure that ozone could react well with NO molecules. Increasing ozone injection rate resulted in reduced NO concentration which NO was oxidised and formed NO_2 as shown in Figure 7A. Based on the linear equation obtained from the results, to completely oxidise NO into NO_2, 4.572 g/h of O_3 is required which corresponds to O_3/NO ratio of 6.145 (Figure 7B). According to the stoichiometry of NO + O_3 $\rightarrow$ NO_2 + O_2 reaction, only O_3/NO ratio of 1.0 is needed [25]. However, in practice, approximately 5 times more of O_3/NO ratio was needed to realise complete NO oxidation which was due to high flue gas temperature that caused O_3 decomposition via O + O_2 $\leftrightarrow$ O_3 and O_3 + O $\rightarrow$ O_2 pathways. The short residence time (831 ms) for the O_3 to react with NO in the flue gas stream was the main reason for the need to use an excessive amount of O_3. If high rate of O_3 injection is performed and O_3/NO ratio is further enhanced, NO_2 can be oxidised into higher NOx such as NO_3 which ultimately form N_2O_5 as end-product through NO_2 + NO_3 $\rightarrow$ N_2O_5 reaction. This is an important step for improving NOx removal applications using alkaline solution [27]. For application to enhance fast-SCR reaction, only 50% of NO in flue gas would be needed to oxidise into NO_2 to obtain NO_2/NO ratio equals 1. Based on Figure 7C, it results in 1.748 g/h of ozone needed which corresponds to O_3/NO of 2.35 and NO conversion efficiency of approximately 1.0 g/kWh as depicted in Figure 7D. The lowered O_3/NO ratio means the smaller excess ozone required and higher system's efficiency can be realised.

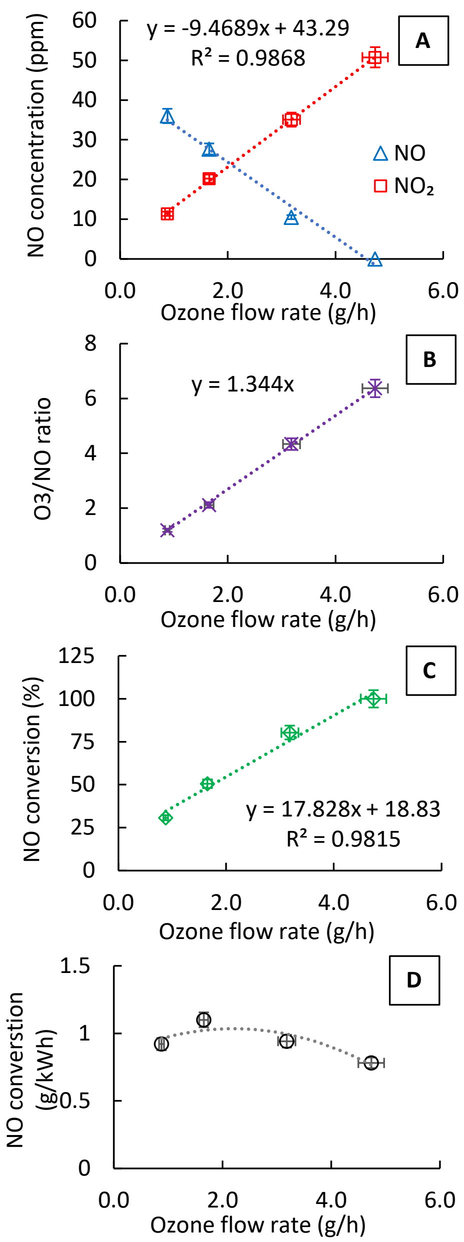

Fig. 7. Effect of input ozone flow rate on NOx emission characteristics at flue gas flow rate of 270 LPM.

Figure 8 demonstrates the effect of flue gas flow rate on NOx emission characteristics when constant ozone injection of 3.3 g/h was supplied to the flue gas stream. The greater flue gas flow rate means higher number of NO molecules introduced at given duration as depicted in Figure 8A which effectively reduced O_3/NO ratio as depicted in Figure 8B. As a result, higher amounts of unconverted NO could be observed because of significant lower O_3 flow rate compared to NO molar flow rate. This was reflected in the NO_2 flow rate shown in Figure 8A. The higher flue gas flow rate resulted in a higher flue gas temperature due to the shorter time for the hot gas within the flue gas pipe limits heat transfer to the pipe wall, thereby effectively minimising heat loss.

Figure 8C illustrates the invert correlation between flue gas temperature and its time of residence in the reaction zone section. The combination of high temperature flue gas and increased flue gas flow rate that decreased O_3/NO ratio resulted in larger amount of NO introduced, more O_3 destruction [23] and reduced NO_2 formation. At given O_3 injection rate, flue gas flow rate of 750 LPM demonstrated NO conversion of 50% with the peak NO conversion efficiency of 2.93 g/kWh. Further increase the flue gas flow rate will lead to NO conversion (both % and g/kWh) reduction as illustrated in Figure 8D.

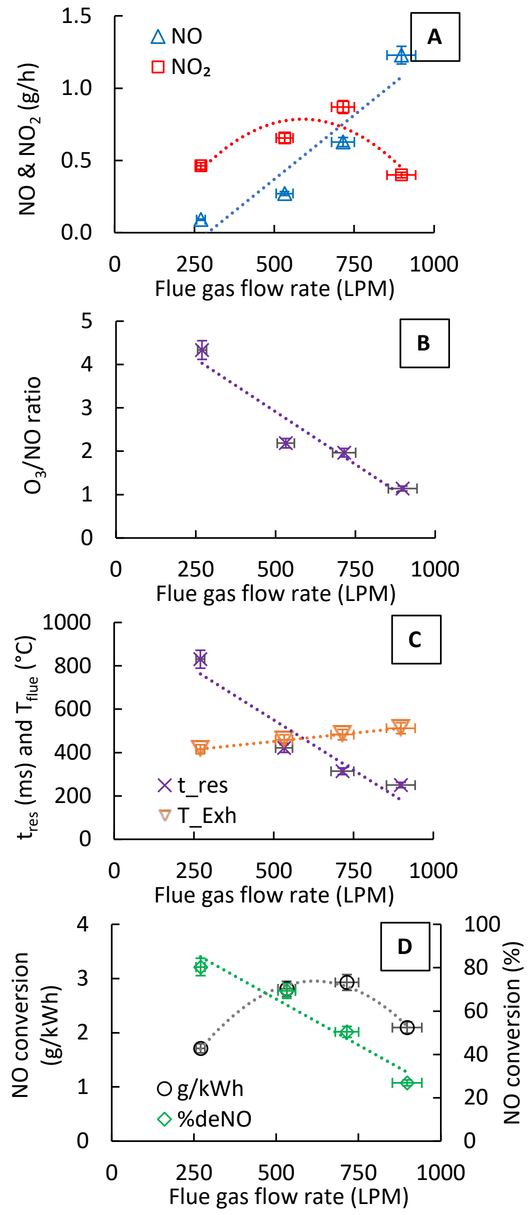

Fig. 8. Effect of flue gas flow rate on NOx emission characteristics at constant ozone injection rate.

4 Conclusions

This work experimentally investigated the effect of real flue gas at elevated temperature and volumetric flow rate on NO oxidation into NO_2 by means of injecting O_3. Ozone production characteristic of the in-house built DBD reactor fed with various concentration of oxygen and high voltage discharge conditions were evaluated. The proposed DBD reactor could reach the maximum ozone yield of 44.08 g/kWh with 100% oxygen feed. The generated O_3 was injected into the flue gas stream generated by a diesel oil burner to evaluate NO conversion to NO_2. The findings reveal that flue gas temperature played a significant role on O_3 destruction which reduced O_3 to react with NO. The higher flue gas flow rate reduces the gas residence time, which minimised heat loss through the flue gas duct. The optimised flue gas flow rate could enhance NO conversion by balancing between minimising O_3 destruction and maximising resident time for the reaction. Consequently, an excess O_3/NO ratio was required to achieve complete oxidation of NO into NO_2, in this case; O_3/NO ratio > 6 was required to entirely oxidise NO. The findings in this study can help NOx aftertreatment engineers to improve the operating condition of NO oxidation system using ozone to enhance SCR performance in real world conditions. Further investigation on NO oxidation using in-situ analytic tools will shed light on the underlying NO to NO_2 mechanisms.

This research budget was allocated by National Science, Research and Innovation Fund (NSRF), and King Mongkut's University of Technology North Bangkok (Project No. KMUTNB-FF-68-B-26).

References

1. T. Skytt, S. N. Nielsen, B.-G. Jonsson, Global warming potential and absolute global temperature change potential from carbon dioxide and methane fluxes as indicators of regional sustainability – A case study of Jämtland, Sweden. *Ecol. Indic.* **110**, 105831 (2020). https://doi.org/10.1016/j.ecolind.2019.105831
2. Y. B. Zeldovich, ZELDOVICH 1959. *Zh. Eksp. Teor. Fiz.* **36**, 964 (1959)
3. D. Erdemir, I. Dincer, A perspective on the use of ammonia as a clean fuel: Challenges and solutions., *John Wiley & Sons. Inc. Chichester, UK.*, 2021
4. H. Xiao, A. Valera-Medina, P. J. Bowen, Study on premixed combustion characteristics of co-firing ammonia/methane fuels. *Energy*. (2017). https://doi.org/10.1016/j.energy.2017.08.077
5. I. Nova, E. Tronconi, Urea-SCR Technology for deNOx After Treatment of Diesel Exhausts. *Johnson Matthey Technol. Rev.* **59**, 221–232 (2014). https://doi.org/10.1007/978-1-4899-8071-7
6. R. Villamaina, I. Nova, E. Tronconi, T. Maunula, M. Keenan, Effect of the NH4NO3 Addition on the Low-T NH3-SCR Performances of Individual and Combined Fe- and Cu-Zeolite Catalysts. *Emiss. Control Sci. Technol..* **5**, 290–296 (2019). https://doi.org/10.1007/s40825-019-00140-3
7. C.-N. Kuo, C.-S. Li, Y.-L. Lai, S.-I. Yen, Metal-Doped Mesoporous MnO2-CeO2 Catalysts for Low-Temperature Pre-Oxidation of NO to NO2 in Fast SCR Process. (2023). https://doi.org/10.3390/catal13040694
8. W.-J. Li, T.-Y. Li, M.-Y. Wey, Preferred enhancement of fast-SCR by Mn/CeSiOx catalyst: Study on Ce/Si promotion and shape dependence. *Chem. Eng. J.* **403**, 126317 (2021). https://doi.org/10.1016/j.cej.2020.126317
9. M. Okubo, T. Kuwahara, Chapter 3 - Principle and design of emission control systems. M. Okubo and T. B. T.-N. T. for E. C. in M. D. E. Kuwahara, Eds. Butterworth-Heinemann. 53–143. (2020). https://doi.org/10.1016/B978-0-12-812307-2.00003-1
10. M. Okubo, T. Kuwahara, Chapter 4 - Operation examples of emission control systems. M. Okubo and T. B. T.-N. T. for E. C. in M. D. E. Kuwahara. Eds. Butterworth-Heinemann. 145–210. (2020). https://doi.org/10.1016/B978-0-12-812307-2.00004-3
11. N. Osawa, T. Tsuji, R. Ogiso, Y. Yoshioka, Effect of nitrogen addition to ozone generation characteristics by diffuse and filamentary dielectric barrier discharges at atmospheric pressure*. *Eur. Phys. J. Appl. Phys.* **78**, (2017). [Online]. Available: https://doi.org/10.1051/epjap/2017160471
12. K.-M. Lin, T.-Y. Liao, J.-Y. Lin, M. Abrar, Y.-X. Chen, Analysis of ozone generation in a planar atmospheric pressure air dielectric barrier discharge reactor. *Plasma Sources Sci. Technol.* **32**, 25007 (2023). https://doi.org/10.1088/1361-6595/acb812
13. M. Tański, A. Reza, D. Przytuła, K. Garasz, Ozone Generation by Surface Dielectric Barrier Discharge. *Appl. Sci.* **13**, (2023). https://doi.org/10.3390/app13127001
14. L. Wei, H. Deng, G. Neretti, Y. Zhang, Ozone yield limit in low temperature plasmas based on thermodynamics. *Eur. Phys. J. D.* **73**, 136 (2019). https://doi.org/10.1140/epjd/e2019-90560-y
15. M. Zhang *et al.*, Intensification of NOx Conversion over Activated Coke by Ozone Oxidation for Sintering Flue Gas at Low Temperatures. *ACS Omega.* **6**, 13484–13495 (2021). https://doi.org/10.1021/acsomega.1c01722
16. Y. Nie, L. Xu, Y. Yang, D. He, Y. Mei, Mechanism investigation on yellow phosphorus inducing O, O3 and OH• radicals in phosphate rock slurry for high-efficiency NO oxidation. *Sep. Purif. Technol.* **312**, 123435 (2023). https://doi.org/10.1016/j.seppur.2023.123435
17. L. Liu, B. Shen, M. Si, F. Lu, Performance and mechanism of MnOx/γ-Al2O3 for low-temperature NO catalytic oxidation with O3/NO ratio of 0.5. *Fuel Process. Technol.* **222**, 106979 (2021). https://doi.org/10.1016/j.fuproc.2021.106979
18. Z. Zhang, H. Xi, S. Zhou, W. Zhou, M. Shreka, Efficient removal of NOx from simulated marine exhaust by using O3-Na2SO3: Experimental factors and optimization analysis. *Fuel.* **313**, 122659 (2022). https://doi.org/10.1016/j.fuel.2021.122659

19. F. Meng *et al.*, Promotional effect of surface fluorine on TiO2: Catalytic conversion of O3 and H2O2 into ·OH and ·O2− radicals for high-efficiency NO oxidation. *Chem. Eng. J.* **424**, 130358 (2021). https://doi.org/10.1016/j.cej.2021.130358
20. S. Bhowmick, A. Badiwal, K. T. Shenoy, Removal of NOx using ozone injection and subsequent absorption in water. *Chem. Eng. J. Adv.* **15**, 100511 (2023). https://doi.org/10.1016/j.ceja.2023.100511
21. M. Holub, S. Kalisiak, T. Borkowski, J. Myskow, R. Brandenburg, The Influence of Direct Non-Thermal Plasma Treatment on Particulate Matter (PM) and NOx in the Exhaust of Marine Diesel Engines. *Polish J. Environ. Stud.* **19**, 1199–1211 (2010). [Online]. Available: http://apps.webofknowledge.com/full_record.do?product=UA&search_mode=GeneralSearch&qid=1&SID=R2NLPhmYMEEtpS9Gxa8&page=1&doc=9
22. H. Yamasaki *et al.*, Pilot-Scale NOx and SOx Aftertreatment by Semi-Dry Plasma-Chemical Hybrid Process in Glass-Melting-Furnace Exhaust Gas. *Plasma Chem. Plasma Process.* **42**, 51–71 (2022). https://doi.org/10.1007/s11090-021-10193-4
23. S. Jodzis, M. Zięba, Energy efficiency of an ozone generation process in oxygen. Analysis of a pulsed DBD system. *Vacuum*. **155**, 29–37 (2018). https://doi.org/10.1016/j.vacuum.2018.05.035
24. R. A. Bryant, Uncertainty estimates of tracer gas dilution flow measurements in large-scale exhaust ducts. *Flow Meas. Instrum.* **61**, 1–8 (2018). https://doi.org/10.1016/j.flowmeasinst.2018.03.004
25. M. Si *et al.*, Review on the NO removal from flue gas by oxidation methods. *J. Environ. Sci.*, **101**, 49–71 (2021). https://doi.org/10.1016/j.jes.2020.08.004
26. K.-M. Lin, K.-C. Wang, Y.-S. Chang, S.-Y. Chuang, Gas Heating Mechanisms in Atmospheric Pressure Helium Dielectric-Barrier Discharges Driven by a kHz Power Source. (2020). https://doi.org/10.3390/app10217583
27. Z. Zhu, B. Xu, Purification Technologies for NOx Removal from Flue Gas: A Review. (2022). https://doi.org/10.3390/separations9100307